Conformational and Quantitative Structure−Activity Relationship Study of Cytotoxic 2-Arylidenebenzocycloalkanones

Jonathan R. Dimmock,*,† N. Murthi Kandepu,† Adil J. Nazarali,† Travis P. Kowalchuk,† Narasimhan Motaganahalli,† J. Wilson Quail,‡ Patricia A. Mykytiuk,§ Gerald F. Audette,§ Lata Prasad,§ Pál Perjési,*,|| Theresa M. Allen,⊥ Cheryl L. Santos,⊥ Jen Szydlowski,⊥ Erik De Clercq,▽ and Jan Balzarini▽

College of Pharmacy and Nutrition and Departments of Chemistry and Biochemistry, University of Saskatchewan, Saskatoon, Saskatchewan S7N 5C9, Canada, Department of Medical Chemistry, University Medical School of Pécs, H-7624 Pécs, Hungary, Department of Pharmacology, University of Alberta, Edmonton, Alberta T6G 2H7, Canada, and Rega Institute for Medical Research, Katholieke Universiteit Leuven, B-3000 Leuven, Belgium

Received November 25, 1998

Various 2-arylideneindanones **1**, 2-arylidenetetralones **2**, and 2-arylidenebenzosuberones **3** were synthesized with the aim of determining the relative orientations of the two aryl rings which favored cytotoxicity. Molecular modeling of the unsubstituted compound in each series revealed differences in the spatial arrangements of the two aryl rings, and evaluation of these compounds against P388, L1210, Molt 4/C8, and CEM cells as well as a panel of human tumor cell lines indicated that in general the order of cytotoxicity was **3** > **2** > **1**. In particular 2-(4-methoxyphenylmethylene)-1-benzosuberone (**3k**) had the greatest cytotoxicity, possessing 11 times the potency of the reference drug melphalan when all five screens were considered. Series **3** was considered in further detail. First, excision of the aryl ring fused to the cycloheptanone moiety in series **3** led to some 2-arylidene-1-cycloheptanones **4** which had approximately one-third of the bioactivity of the analogues **3**. Second, in some screens cytotoxicity was correlated negatively with the σ values and positively with the MR constants of the substituents in the arylidene aryl ring of **3**. Third, X-ray crystallography of five representative compounds (**3i,k**−**n**) revealed differences in the locations of the aryl rings which may have contributed to the variations in cytotoxicity. Finally three members of series **3** inhibited RNA and protein syntheses and induced apoptosis in human Jurkat T cells. This study has revealed that 2-arylidene-1-benzosuberones are a group of useful cytotoxic agents, and in particular **3k** serves as a prototypic molecule for subsequent structural modifications.

Introduction

A major interest of these laboratories is the design, syntheses, and evaluation of conjugated styryl ketones and related compounds as candidate cytotoxic and anticancer agents.[1,2] A number of these compounds displayed a marked affinity for the mercapto groups of various naturally occurring thiols and did not react with amino or hydroxy groups.[3,4] These latter two substituents are present in nucleic acids, and hence α,β-unsaturated ketones may not have the genotoxic effects which are associated with various alkylating agents used in cancer chemotherapy.[5]

The objectives of the present study were as follows. For a number of years, the cytotoxic and anticancer properties of chalcone (1,3-diphenyl-2-propenone) and related compounds have been documented.[6−8] These compounds are conjugated molecules, but they are still sufficiently flexible to permit a wide variety of conformations. Hence discernment of the optimal shapes of these molecules displaying cytotoxic activity is not possible. In particular, the spatial arrangement of the two aryl rings would be expected to influence bioactivity profoundly. Thus the preparation of rigid analogues of chalcones, namely, series **1**−**3**, was contemplated in which the locations of the two aryl rings could vary from one series to another. The cytotoxic evaluation of these compounds should permit some understanding of the importance of the relative positions of the aryl rings. This concept is illustrated for the unsubstituted compounds **1a**, **2a**, and **3a** in Figure 1. To explore the generality of this approach, identical substituents were placed in the arylidene rings in each of the three series of compounds. If the principal, or possibly sole, mechanism of action is the same for all compounds in series **1**−**3**, then differences in cytotoxicity may be attributed to variation in the shapes of the three groups of compounds.

A second objective of this study was to seek correlations between the electronic, hydrophobic, and steric properties of the aryl substituents in the series demonstrating the greatest bioactivity with a view to determining those physicochemical parameters which contribute to cytotoxicity. A wide range of nuclear substituents were chosen; in fact the groups are found in three of the four quadrants of a Craig plot.[9] In addition, the data generated may serve to develop structure−activity relationships which may afford directions for the development of novel cytotoxic and anticancer agents.

In summary therefore, the initial phase of the study was to prepare the compounds in series **1**−**3** for evalu-

* Correspondence may be directed to either author.
† College of Pharmacy and Nutrition, University of Saskatchewan.
‡ Department of Chemistry, University of Saskatchewan.
§ Department of Biochemistry, University of Saskatchewan.
|| University Medical School of Pécs.
⊥ University of Alberta.
▽ Katholieke Universiteit Leuven.

10.1021/jm9806695 CCC: $18.00
Published on Web 04/02/1999

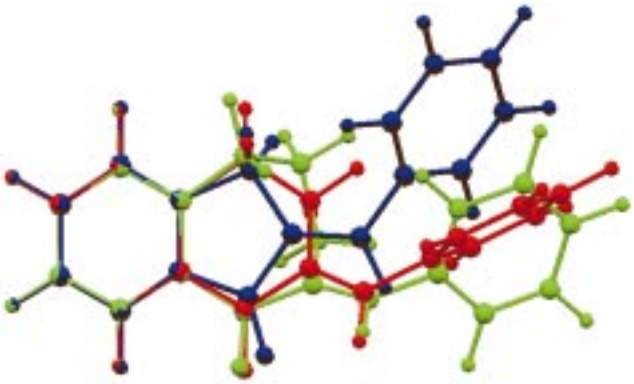

Figure 1. Comparison of the shapes of **1a** (blue), **2a** (red), and **3a** (green) generated by molecular modeling in which the six carbon atoms of the aryl ring fused to the alicyclic ring were overlapped.

Chart 1. Structures of compounds **1**−**4**[a]

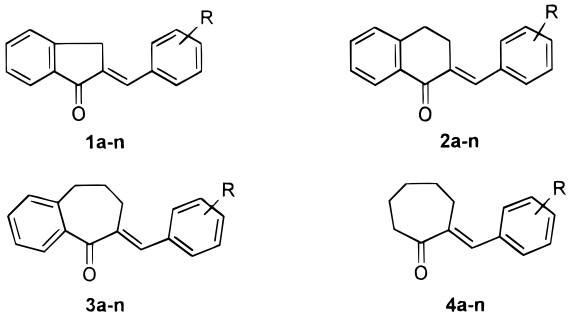

[a] Substituents: **a**, R = H; **b**, R = 3-F; **c**, R = 4-F; **d**, R = 3-Cl; **e**, R = 4-Cl; **f**, R = 3-Br; **g**, R = 4-Br; **h**, R = 3-CH_3; **i**, R = 4-CH_3; **j**, R = 3-OCH_3; **k**, R = 4-OCH_3; **l**, R = 3-NO_2; **m**, R = 4-NO_2; **n**, R = 4-$N(CH_3)_2$.

ation against different murine and human malignant cells. The principal objective was to gain some indication of the preferable orientation of the aryl rings in these molecules and also to discern the effects of different aryl substituents on cytotoxicity.

Chemistry

The unsaturated ketones **1**−**3** (Chart 1) were prepared by a Claisen−Schmidt condensation between 1-indanone, 1-tetralone, or 1-benzosuberone and the appropriate aryl aldehyde. The 2-arylidene-1-cycloheptanones **4** vide infra were synthesized either by the same route (**4a**−**k**) or by reaction of 4-morpholinyl-1-cycloheptene with various aryl aldehydes (**4l**−**n**).

The infrared spectra of the enones in series **1**−**4** were determined. Each compound exhibited a single strong absorption for the carbonyl group denoting its stereochemical homogeneity. The carbonyl absorptions for series **1**−**4** were noted in the regions of 1679−1696, 1658−1666, 1651−1664, and 1665−1684 cm^{-1}, respectively. The higher wavenumbers in series **1** compared to the analogues in **2** and **3** may be attributed to the ring strain in **1**. The lower carbonyl stretching frequencies of series **3** compared to **4** indicated the contribution of the aryl ring A to conjugation in the 2-arylidene-1-benzosuberones. (For the designation of the aryl rings as A and B, see Figure 2.)

The ^1H NMR spectra of solutions of the compounds in series **1**−**4** were determined. The aliphatic methine protons of the enones in series **1**−**3** appeared in the

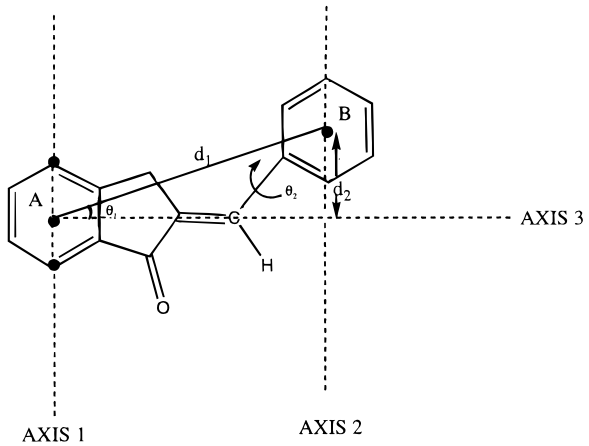

Figure 2. Distances and bond angles of **1a**.

region of 7.15−7.95 ppm; these absorptions were at low field due to the proximity of the carbonyl group (see Figure 1) which exerted an anisotropic effect. For this reason, the methine protons are shifted downfield and frequently overlapped with the complex multiplet arising from the aromatic protons. Previous studies revealed that the methine absorptions of the *E* and *Z* isomers of 2-(phenylmethylene)-3,3-dimethyl-1-indanone were 7.65 and 6.80 ppm[10,11] and the relevant data for 2-(phenylmethylene)-4,4-dimethyl-1-tetralone were 7.71 and 6.63 ppm, respectively.[11] In the case of the 2-arylidene-1-benzosuberones **3a**−**l**,**n**, the methine protons and those of the condensed benzene ring in the *peri* position to the carbonyl group are overlapped in the region of 7.65−7.95 ppm. These two protons as well as the other three aromatic protons in **3m** appeared at 7.05−7.95 ppm. These values are in accord with the published data for the *E* isomer of **3a**.[12] The aliphatic methine proton in series **4** was found in the region of 7.05−7.80 ppm. Since the corresponding absorptions for the *E* and *Z* isomers of 2-(phenylmethylene)-6,6-diphenylcyclohexanone are 7.00−7.50 and 6.33 ppm, respectively,[13] the compounds in series **4** (as well as in series **1**−**3**) were assigned the *E* configuration. Detailed infrared and ^1H and ^{13}C NMR investigations on selected derivatives of series **1**−**3**[14] and **4**[15] provided further evidence for the stereohomogeneity and *E* configuration of the compounds.

To compare the shapes of the compounds in series **1**−**3**, molecular models of **1a**, **2a**, and **3a** were built and the aryl ring fused to the alicyclic rings was superimposed as illustrated in Figure 1. In addition, X-ray crystallography was undertaken on **3i,k**−**n**, and superimposition of the fused aryl ring of all five compounds revealed that different orientations of the rest of the molecules occurred. This result is displayed in Figure 3. Certain distances and angles were measured as illustrated in Figure 2. These data from both the molecular modeling and X-ray crystallographic studies are displayed in Tables 1 and 5, respectively.

Cytotoxicity and Biochemical Screens

The compounds in series **1**−**4** were evaluated against murine P388 and L1210 leukemic cells as well as human Molt 4/C8 and CEM T-lymphocytes. These data are presented in Table 2. The cytotoxicity of various α,β-unsaturated ketones toward a number of human tumor cell lines was determined, and the results are portrayed

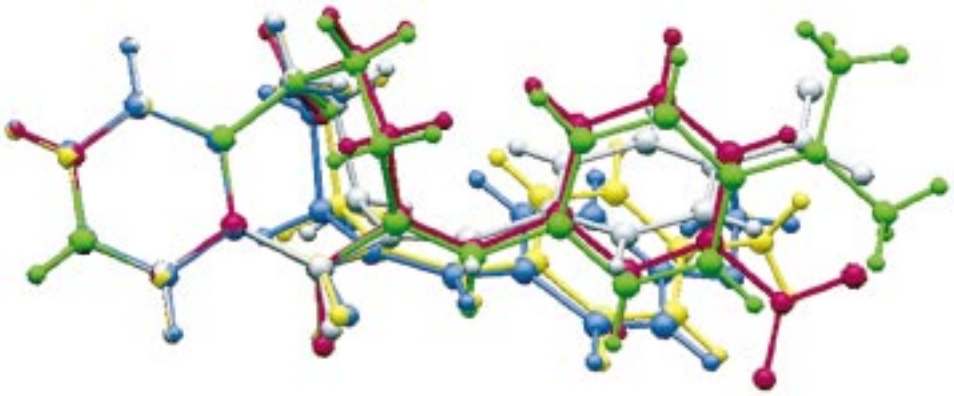

Figure 3. Comparison of the shapes of **3i** (yellow), **3k** (blue), **3l** (red), **3m** (gray), and **3n** (green) determined by X-ray crystallography in which the six carbon atoms of the aryl ring fused to the alicyclic ring were overlapped.

Table 1. Various Distances and Angles of **1a**, **2a**, and **3a** Found by Molecular Modeling

compd	d_1 (Å)	d_2 (Å)	θ_1 (deg)	θ_2 (deg)[a]
1a	6.85	2.14	18.2	58.7
2a	7.47	0.18	1.4	−58.6
3a	7.43	1.4	10.9	85.2

[a] The signs of the torsion angles are positive or negative if the rotation is anticlockwise or clockwise, respectively.

in Table 4. Compounds **3i,k,n** inhibited RNA and protein syntheses as well as induced apoptosis in human Jurkat T cells; these data are summarized in Table 6.

Results and Discussion

The spatial orientations of the two aryl rings in these enones were compared by building models of three representative compounds in each series, namely, **1a**, **2a**, and **3a**. A conformational search of these three compounds used the Monte Carlo method, and 1000 starting conformations for each of the three compounds were minimized. The conformations reported have the lowest energy with the maximum number of original conformations reaching this energy minima. The conformations with the next higher minimum energy had similar shapes except for the θ_2 figures vide infra. In this representation, the six carbon atoms of the aryl ring fused to the alicyclic ring were superimposed, which is illustrated in Figure 1. A difference between the location of the arylmethylene ring in **1a** and the other two compounds was observed which may contribute to variations in the cytotoxicities between the enones in series **1** and those found in series **2** and **3**. Furthermore the figures indicate that the rings in **2a** and **3a** are orientated in a different manner which may have an impact on bioactivity.

To quantify some of the differences between the orientations of the two aryl rings of **1a**, **2a**, and **3a**, certain distances and angles were measured. The following approach was adopted and is illustrated in Figure 2. Initially carbon atoms were placed in the centers of rings A and B which will be referred to hereafter as C_A and C_B. Axis 1 was constructed by incorporating C_A and two other carbon atoms of ring A as illustrated in Figure 2. Axis 2 was constructed in a similar manner in ring B. Axis 3 was made at right angles to axis 1 and perpendicular to axis 2. The distances between the centers of rings A and B (d_1) and also the elevation (or depression) of ring B above (or below) axis 3, i.e., d_2, were measured. This deviation from coplanarity of rings A and B was also calculated by measuring θ_1. Finally the possible lack of coplanarity of ring B with the adjacent unsaturated linkage (θ_2) was determined. The results are summarized in Table 1.

The following differences in shape between the three compounds were noted, each of which may influence bioactivity. First, rings A and B are closest in **1a**, and the d_1 distance is increased by 9% in the case of **2a** and **3a**. Second, the d_2 and θ_1 figures revealed that the centers of both aromatic rings in **2a** are virtually in the same plane in contrast to the centers of rings B in **1a** and **3a** which are above the plane of rings A. Finally, the θ_2 values demonstrated that the aryl rings B of **1a** and **2a** were approximately 59°, while the torsion angle of **3a** was 45% greater, i.e., 85°. These differences in spatial orientations of the two aryl rings are considered to play an important part in the variation in cytotoxic activity in series **1**−**3** (see Table 3 and the relevant discussion in the text).

The cytotoxic properties of the compounds in series **1**−**3** against two murine leukemias and two human T-lymphocytes are presented in Table 2. The highest concentration of compound used in the P388 screen was 50 μM. Since the other cell lines were, in general, less sensitive to these ketones, a 10-fold increase in the magnitude of the highest concentrations, i.e., 500 μM, was used in the L1210, Molt 4/C8, and CEM screens. To compare the cytotoxicity of the enones in series **1**−**3** with a view to determining which spatial arrangement favored bioactivity, the following approach was adopted. When the IC_{50} values were greater than 50 μM (P388 screen) or 500 μM (in the case of the other cell lines), these figures of 50 or 500 μM were used in computing the average cytotoxicity for a series of compounds. Hence the term average potency (AP) will be used since the figures generated are not strictly IC_{50} figures. These data are summarized in Table 3.

In the case of the evaluation using P388 cells, the figures in Table 3 revealed that the order of potency in the three series was **3** > **2** > **1**. In series **1** only 36% of the compounds had IC_{50} figures of less than 50 μM (see Table 2) and were clearly markedly less active than the corresponding six- and seven-membered cycloalkanones **2** and **3**. In addition, comparisons were made between the analogues having the same substituents in the aryl rings, e.g., the potencies of **1a, 2a,** and **3a** were contrasted and the IC_{50} figures of **1k, 2k,** and **3k** were

Table 2. Evaluation of the Compounds in Series **1**−**4** against Murine P388 and L1210 Leukemic Cells and Human Molt 4/C8 and CEM T-Lymphocytes

	IC_{50} (μM)			
compd	P388 cells	L1210 cells	Molt 4/C8 cells	CEM cells
1a	>50	112 ± 52	42.3 ± 5.9	41.3 ± 0.8
1b	40.0	181 ± 17	46.1 ± 7.2	39.2 ± 1.8
1c	>50	89.0 ± 39.6	60.0 ± 11.7	42.2 ± 5.2
1d	26.3	41.2 ± 10.1	50.9 ± 11.7	31.8 ± 13.4
1e	>50	54.1 ± 0.3	>500	284 ± 141
1f	21.0	43.3 ± 2.6	173 ± 115	32.4 ± 24.0
1g	>50	64.8 ± 2.7	>500	299 ± 193
1h	24.9	50.4 ± 13.9	80.3 ± 18.0	41.3 ± 10.1
1i	38.6	59.1 ± 2.5	>500	67.1 ± 18.9
1j	>50	217 ± 38	>500	>500
1k	>50	45.8 ± 0.3	226 ± 59	32.6 ± 14.5
1l	>50	256 ± 35	>500	222 ± 53
1m	>50	>500	>500	>500
1n	>50	61.7 ± 2.2	135 ± 84	41.0 ± 22
2a	30.2	121 ± 104	32.4 ± 16.6	7.42 ± 0.56
2b	31.1	61.2 ± 3.5	11.9 ± 1.5	8.01 ± 0.78
2c	15.9	49.3 ± 0.0	41.2 ± 1.3	33.4 ± 3.3
2d	16.8	118 ± 97	41.8 ± 0.8	9.19 ± 0.92
2e	20.9	69.1 ± 21.8	>500	48.2 ± 10.6
2f	16.6	158 ± 164	21.2 ± 4.9	8.79 ± 0.93
2g	20.4	202 ± 172	>500	>500
2h	16.3	73.2 ± 37.8	35.8 ± 2.2	9.41 ± 0.50
2i	17.7	161 ± 159	>500	460 ± 69
2j	17.6	60.7 ± 21.8	12.1 ± 2.0	8.78 ± 0.29
2k	22.1	44.0 ± 2.9	9.41 ± 0.29	8.84 ± 0.22
2l	12.0	254 ± 22	8.01 ± 0.30	5.30 ± 0.64
2m	>50	>500	>500	>500
2n	5.3	17.5 ± 6.7	2.11 ± 0.36	1.65 ± 0.08
3a	12.7	106 ± 31	42.7 ± 3.3	28.9 ± 0.7
3b	10.9	134 ± 50	28.3 ± 2.4	11.2 ± 2.6
3c	11.1	60.3 ± 10.6	53.6 ± 7.0	20.0 ± 6.4
3d	8.2	52.3 ± 0.0	23.8 ± 2.7	9.44 ± 2.06
3e	9.5	51.8 ± 0.4	33.0 ± 0.3	15.1 ± 4.7
3f	10.5	51.0 ± 3.5	17.1 ± 0.3	8.90 ± 0.90
3g	18.6	50.9 ± 0.1	54.7 ± 4.7	17.1 ± 1.5
3h	19.9	54.4 ± 5.7	34.6 ± 1.1	15.8 ± 4.8
3i	11.8	25.0 ± 7.4	21.3 ± 14.1	11.4 ± 1.6
3j	13.9	56.3 ± 1.8	>100[a]	9.50 ± 0.16
3k	1.6	0.34 ± 0.02	0.47 ± 0.33	0.35 ± 0.04
3l	15.8	48.8 ± 0.2	8.82 ± 0.38	7.72 ± 0.93
3m	10.9	>500	>500	>500
3n	1.9	1.87 ± 0.07	5.25 ± 3.63	3.05 ± 0.46
4a	>50	261 ± 18	215 ± 10	110 ± 22
4b	>50	382 ± 85	482 ± 25	224 ± 23
4c	>50	291 ± 32	250 ± 59	198 ± 1
4d	25.7	144 ± 19	88.6 ± 20.3	40.5 ± 1.9
4e	19.1	83.0 ± 16.4	52.6 ± 4.0	43.5 ± 0.5
4f	24.1	246 ± 19	176 ± 8	137 ± 15
4g	16.8	68.4 ± 11.8	49.4 ± 8.7	42.8 ± 0.4
4h	29.8	263 ± 33	228 ± 50	170 ± 32
4i	>50	>500	>500	>500
4j	>50	283 ± 33	170 ± 32	128 ± 6
4k	>50	306 ± 30	250 ± 13	194 ± 3
4l	23.6	162 ± 36	39.2 ± 4.1	30.1 ± 0.7
4m	25.2	104 ± 6	39.6 ± 1.5	36.3 ± 5.4
4n	18.8	79.1 ± 12.9	57.4 ± 14.1	45.1 ± 5.6
melphalan	0.22	2.13 ± 0.03	3.24 ± 0.79	2.47 ± 0.30

[a] At a concentration of 500 μM, **3j** is insoluble in the cell culture.

Table 3. Average Potency (AP, μM)[a] for Series **1**−**4** Using Different Murine and Human Cell Lines

series	P388 cells	L1210 cells	Molt 4/C8 lymphocytes	CEM lymphocytes
1	42.9 (21.0−50)	127 (41.2−500)	267 (42.3−500)	155 (31.8−500)
2	20.9 (5.3−50)	135 (17.5−500)	158 (2.11−500)	115 (1.65−500)
3	11.2 (1.6−19.9)	85.2 (0.34−500)	66.0 (0.47−500)	47.0 (0.35−500)
4	34.5 (16.8−50)	227 (68.4−500)	186 (39.2−500)	136 (30.1−500)

[a] The term average potency is defined in the Results and Discussion section.

compared. In 11 of the 14 comparisons, the potencies were in the order of **3** > **2** > **1**, and in all cases the compounds in **3** were more cytotoxic than the analogues in series **1**. In general, the ketones were less active toward the more rapidly growing L1210 cells than the somewhat slower growing P388 leukemia cells. The AP

Table 4. Cytotoxicities of Various Cyclic Enones toward Human Tumor Cell Lines

compd	MG MID[a] (μM)	compd	MG MID[a] (μM)
1f	46.7	**4a**	91.2
1l	91.2	**4b**	67.6
2f	11.8	**4c**	83.2
3a	18.6	**4d**	41.7
3b	16.2	**4e**	33.1
3d	16.6	**4h**	81.3
3e	17.0	**4i**	83.2
3h	20.0	**4j**	85.1
3i	11.2	**4k**	100
3j	15.9	**4l**	30.2
3k	0.269	**4m**	30.2
3l	10.2	**4n**	85.1
3m	89.1	melphalan	25.7
3n	1.41		

[a] The letters MG MID refer to the mean graph midpoint values. This term is explained in the Results and Discussion section.

Table 5. Various Distances and Angles of **3i,k**−**n** Found from X-ray Crystallography

compd	d_1 (Å)	d_2 (Å)	θ_1 (deg)	θ_2 (deg)[a]
3i	7.74	2.18	16.4	25.1
3k	7.47	2.18	17.0	19.1
3l	7.72	1.46	10.9	−30.3
3m	7.68	0.78	5.8	6.0
3n	7.74	2.13	16.0	−22.9

[a] The signs of the torsion angles are positive or negative if the rotation is anticlockwise or clockwise, respectively.

figures in Table 3 indicated that in the L1210 screen, while series **3** had the highest activity, series **1** was slightly more potent than the compounds in series **2**. In comparing the data for the enones when the aryl substituents were identical, the greatest cytotoxicities were found in eight, two, and three times in series **3**, **2**, and **1,** respectively.

The figures in Table 3 revealed that the relative cytotoxicity of the unsaturated ketones toward Molt 4/C8 T-lymphocytes was in the order of **3** > **2** > **1**. When compounds with the same aryl substituents were compared, the greatest cytotoxicity was displayed almost equally by the compounds in series **3** and **2** and on no occasion by the analogues in series **1**. In general, the ketones **1**−**3** were more active against the CEM cells than toward the Molt 4/C8 lymphocytes. The data in Table 3, obtained using CEM cells, indicated an order of potency of **3** > **2** > **1**. However in the 13 comparisons with compounds possessing the same aryl substituents, maximum activity was found in 8 of the derivatives in series **2** and 5 in series **3**.

If the hypothesis that the spatial orientations of the aryl rings significantly influence cytotoxicity is valid, then the data indicate that the relative locations of the rings in the 2-arylidenebenzosuberones **3** are preferable to the conformations of these two groups in series **1** and **2**. Thus future design of cytotoxic agents which are rigid or semirigid analogues of chalcones should bear in mind the distances between, and positions of, the two aryl rings in the 2-arylidenebenzosuberones.

The next phase of the work was directed toward discerning those structural features which caused variations in cytotoxicity. To explore further the hypothesis that bioactivity was influenced markedly by the presence and orientation of both aryl rings, series **4** was prepared in which the aryl ring fused to the cycloaliphatic ring in **3** had been excised. The AP figures in Table 3 revealed that the compounds in series **3** had approximately 3 times the activity of the ketones **4** indicating the importance of the presence of an aryl ring attached to the 2-arylidenecycloheptanone moiety.

The IC_{50} figures of the compounds in series **1**−**4** were reviewed in terms of potency by comparing their activities with that of melphalan. In particular, those unsaturated ketones possessing 10% or more of the activities of this antineoplastic drug were noted. In the P388 screen, compounds **3k**,**n** had 14% and 12%, respectively, of the activity of melphalan; the remaining compounds were far less potent. A similar situation prevailed in the L1210 test insofar as the most active compounds were **3k**,**n**. However in this case, these ketones possessed 6.3 and 1.1 times, respectively, the potency of the reference alkylating agent. None of the other ketones had 10% or more of the activity of melphalan. In the case of the human T-lymphocytes, half or more of the compounds in series **2** and **3** had IC_{50} figures corresponding to at least 10% of the activity of melphalan. Using Molt 4/C8 cells **2a**,**b**,**f**,**j**,**k**,**l**,**n** and **3b**,**d**-,**f**,**i**,**k**,**l**,**n** met this criterion. Of these compounds **2n** and **3k** had 1.5 and 6.9 times the activity of melphalan. When CEM cells were employed, **2a**,**b**,**d**,**f**,**h**,**j**,**k**,**l**,**n** and **3b**−**l**,**n** were the most potent compounds and in particular **3k** was 7.1 times more potent than melphalan. One may summarize these data by indicating that **3k**,**n** were the most active compounds toward the murine P388 and L1210 cells and **3k** had the greatest activity toward leukemic cells derived from the T-lymphocytes. A noteworthy feature of the data revealed that **3k** was the most cytotoxic unsaturated ketone in all four screens, and it is clearly a very useful lead molecule.

Representative compounds were also evaluated against approximately 55 human tumor cell lines from nine different neoplastic diseases: leukemia, melanoma, non-small-cell lung, colon, central nervous system, ovarian, renal, prostate, and breast cancers.[16] The ketones were screened using concentrations of log 10^{-4} to log 10^{-8} M, and the amounts of compounds required to inhibit 50% of the growth of the cells were noted. In some cases, the concentration of compound necessary to inhibit 50% of the growth of a particular cell line was greater than the highest concentration used, i.e., log 10^{-4} M, although this figure was incorporated into the average value for all cell lines. Thus the term mean graph midpoint (MG MID) was employed in this screen. The number of cell lines for which actual IC_{50} figures were obtained is indicated in the Experimental Section. A greater than 50% inhibition of the growth of the neoplastic cells at log 10^{-4} M concentrations was obtained in either all or most cases where the MG MID values were 50 μM or less. In addition to identifying potent cytotoxic agents, a major aim of this screen is to find compounds with selective toxicity for one or more groups of cancers which may permit the identification of compounds with preferential lethality for the same class of neoplasms in vivo.

The results recorded in Table 4 confirmed the general trends using P388, L1210, Molt 4/C8, and CEM cells. First, the 3-bromo unsaturated ketone **1f** had greater cytotoxicity than **1l** but was less potent than the tetralone analogue **2f**. Second, a comparison between the data for **3a**,**b**,**d**,**e**,**h**,**k**−**n** and **4a**,**b**,**d**,**e**,**h**,**k**−**n** revealed that with the exception of **3m**, the 2-arylideneben-

Table 6. Cytotoxicity, Inhibition of RNA and Protein Synthesis, and Apoptotic Indices of **3i,k,n** Using Human Jurkat T Cells[a]

compd	IC_{50} (μM)	IC_{80} (μM)	% inhibition of synthesis of RNA (SD)	% inhibition of synthesis of protein (SD)	apoptotic index
3i	14.6	23.3	84.2 (15.2)	46.3 (4.4)	83.1
3k	3.50	5.60	92.3 (4.1)	19.5 (1.8)	85.7
3n	2.53	4.04	81.8 (6.1)	52.5 (4.6)	65.2
melphalan	2.20	3.52	85.1 (8.2)	30.5 (5.8)	63.2
actinomycin D	0.0045	0.0072	63.2 (13.1)	51.8 (13.4)	
cycloheximide	0.93	1.54	93.3 (6.2)	71.9 (6.1)	

[a] The IC_{50}, IC_{80}, and apoptotic index figures were obtained after exposure of the cells to the compounds for 48 h, while inhibition of RNA and protein syntheses was noted after 8 h. The IC_{80} concentrations of the compounds were used in determining the inhibition of RNA and protein syntheses as well as the apoptotic indices.

zosuberones **3** had greater activity than the analogues **4**. Third, with the exception of **3m**, all of the compounds in series **3** had lower MG MID figures than melphalan. The two most potent compounds were **3k**,**n** possessing 96 and 18 times, respectively, the activity of melphalan. This observation, coupled with the data from the previous screens documented in Table 2, confirms the considerable potential of **3k**,**n** as prototypic molecules for future development.

Series **3** possessed the greatest cytotoxicity toward human tumor cell lines, and the question posed was whether selective toxicity toward one or more neoplastic diseases was observed. Examination of the mean graphs[17] revealed that preferential cytotoxicity was displayed by some of the compounds toward colon, breast, and leukemic cells. The fold increase (FI) in selective toxicity was calculated by comparing the average figure of cytotoxicity toward the cell lines in a particular group of cancers with the MG MID values (which is the average value of all cell lines). Compounds were noted with FI figures of 1.50 or higher, i.e., those ketones having a 50% or more increased toxicity to a particular neoplastic disease. The following unsaturated ketones demonstrated selective toxicity (FI figures in parentheses): **3i** (1.57) and **3n** (1.69) to colon cancers, **3k** (2.41) and **3n** (1.53) to breast neoplasms, and **3e** (1.60) and **3l** (2.31) to leukemia. The comparable FI figures using melphalan for colon, breast, and leukemic cancer cell lines are 1.12, 1.03, and 2.97, respectively.

To determine the extent to which the electronic, hydrophobic, and steric properties of the aryl substituents in series **3** influenced cytotoxicity, linear and semilogarithmic plots were made between the IC_{50} and MG MID figures recorded in Tables 2 and 4 with the σ, π, and molar refractivity (MR) values of the aryl groups. Correlations were described as positive if bioactivity increased as the magnitude of the physicochemical constant was elevated and negative if bioactivity was favored when the constants were lowered or had increasing negative values. The p values generated are recorded in the Experimental Section, and the following correlations ($p < 0.1$) noted. Cytotoxicity was negatively correlated with σ values in the case of the murine P388 and L1210 cells as well as human tumors. The MR figures of the aryl groups in series **3** were positively correlated with bioactivity in the case of all cell lines except the human tumor data recorded in Table 4. The hydrophobicity of the aryl substituents was unimportant in eliciting bioactivity since in the case of all of the cell lines there were no correlations between the π values and cytotoxicity. The conclusion to be drawn from this statistical analysis is that future development of series **3** should include the placement of large substituents on the arylidene ring which are electron-donating.

The observation that cytotoxicity was correlated positively with the electron-donating properties of the aryl substituents is noteworthy since such groups will diminish the electrophilicity of the methine carbon atoms. Thus thiol alkylation may not be the principal mode of action of these compounds. It is conceivable that since substituents with negative σ values will increase the electron density of ring B, van der Waals bonding between this ring and a complementary aryl moiety at a binding site may be enhanced.

In concert with the hypothesis stated previously that the shapes of these molecules influence cytotoxicity, the topology of five representative compounds in series **3** was investigated further. The enones **3k**,**n** were chosen because they are the most cytotoxic compounds found in this study, while **3i**,**l** were substantially less potent and **3m** has the lowest activity among the benzosuberones. Taking into consideration the IC_{50} values obtained in the five cytotoxicity screens, the increased potencies of **3k**,**n**,**i**,**l** over **3m** were 525, 119, 20, and 18, respectively, indicating the wide range of bioactivity among these five compounds. However molecular modeling techniques, whereby the six atoms of the aryl ring fused to the alicyclic ring were superimposed, revealed a complete overlap of all compounds except for the aryl substituents. Hence this physicochemical approach did not explain the great disparity of cytotoxicity among **3i**,**k**−**n**.

Thus a second physicochemical technique was employed, namely, X-ray crystallography, with a view to determining whether the crystal structures of **3i**,**k**−**n** revealed molecules with different shapes. The structures of these five compounds are portrayed in Figure 3 in which there was superimposition of the fused aryl rings revealing different orientations of the remaining parts of the molecules. The d_1, d_2, θ_1, and θ_2 figures (obtained in a similar manner described previously) are recorded in Table 5. The distances between the centers of the aryl rings appeared to be unrelated to bioactivity since the d_1 figures for **3i**,**l**,**m**,**n** were very similar. However the distance was slightly shorter in the case of the most active compound **3k**. The data in Table 5 revealed that **3i**,**k**,**n** had the greatest d_2 and θ_1 figures; for **3l** the values were lower, and the smallest figures were recorded with the least active compound **3m**. The two most cytotoxic enones, **3k**,**n**, were among the three compounds with the highest figures. In general therefore activity is favored by increased deviation of coplanarity of the two aryl rings. In terms of seeking correlations of the θ_2 figures with cytotoxicity, the most

active compounds **3k**,**n** had values of 19−23° which may be optimal in terms of potency. Increases in the θ_2 values were noted in the less active analogues **3i**,**l** and the smallest figure was observed in the least active compound **3m**. One may conclude from the results given in Table 5 that if the shapes of these molecules determined by X-ray crystallography reflect their spatial arrangements in vitro, then the distance d_2 and interplanar angles θ_1 and θ_2 likely influence cytotoxicity. These data afford further guidelines for future molecular modifications not only for the benzosuberones but also for rigid and semirigid analogues of chalcones.

A comparison of the shapes of **3i**,**k**−**n** obtained by molecular modeling, whereby conformational searches provided structures with global minima, and X-ray crystallographic techniques was made. The average d_1, d_2, θ_1, and θ_2 values for these compounds determined by molecular modeling were 7.66 Å, 2.43 Å, 18.5°, and 61.5°, respectively. These figures did not alter when a representative compound (**3k**) was modeled taking into account the effect of solvent molecules (water). The average figures for **3i**,**k**−**n** determined by X-ray crystallography were 7.67 Å, 1.75 Å, 13.2°, and 20.7°, respectively. Hence in very general terms, the molecular modeling and X-ray crystallographic data give approximately similar figures in regard to the distances d_1 and d_2 and the θ_1 angle, while the interplanar angle θ_2 provided by the molecular modeling technique is far greater. Thus the general conclusions regarding the shapes of **1a**, **2a**, and **3a** determined by modeling (with the possible exception of the θ_2 figures) are probably valid although the corresponding information obtained from X-ray crystallography of these compounds would be of interest.

Finally a preliminary investigation into the possible mode(s) of action of representative 2-arylidenebenzosuberones was undertaken. A number of anticancer agents inhibit the synthesis of ribonucleic acid (RNA) and proteins[18] and induce apoptosis.[19,20] A previous investigation from this laboratory showed that human Jurkat T cells were more sensitive to a novel α,β-unsaturated ketone than several other cell lines,[21] and hence this neoplasm was used in the present case. Compounds **3k**,**n** have 26 and 6 times, respectively, the average cytotoxicity of **3i**, and consideration was given to the fact that this variation in cytotoxicity may be correlated with the extent of inhibition of RNA and protein syntheses as well as induction of apoptosis.

The results obtained for **3i**,**k**,**n** and melphalan as well as the established inhibitors of RNA and protein syntheses, namely, actinomycin D and cycloheximide, respectively, are summarized in Table 6. The IC_{50} values of **3i**,**k**,**n** against Jurkat T cells were consistent with the previous cytotoxicity data that **3k**,**n** have greater activity than **3i**. For the apoptosis study vide infra, concentrations of compounds were employed which would cause the death of the majority of the cells; hence IC_{80} figures were generated and also used in the RNA and protein inhibition studies. The data obtained indicated that at the concentrations of compounds utilized, no correlations between inhibition of RNA and protein syntheses and cytotoxicity to Jurkat cells were noted. Thus, all three benzosuberones inhibited RNA synthesis to the same extent, and **3i**,**n** were clearly more potent inhibitors of protein synthesis than **3k**. Cells treated with **3i**,**k**,**n** displayed the characteristic effects of apoptosis which included cell shrinkage, cytoplasmic blebbing, and formation of apoptotic nuclei. An apoptotic index [(number of cells with apoptotic nuclei/number of cells counted) × 100] was calculated for each compound. However no correlation between cytotoxicity and apoptotic indices was observed. The data in Table 6 revealed that some of the ways in which the enones **1**−**4** exert their cytotoxic effects are likely by inhibition of the syntheses of certain macromolecules and inducing apoptosis.

Conclusions

Evaluation of a number of 2-arylidene-1-indanones **1**, 2-arylidene-1-tetralones **2**, and 2-arylidene-1-benzosuberones **3** for cytotoxicity revealed that the greatest activity resided in series **3**. In particular, **3k** is a prototypic molecule serving as a template for subsequent molecular modification with a view to increased activity and selective toxicity for breast neoplasms. A number of physicochemical determinations revealed that the spatial arrangements of the aryl groups influenced cytotoxicity and that the incorporation of substituents into the arylidene aryl ring having negative σ values and positive MR figures increased potency. Data provided from several representative compounds indicated that these enones inhibit RNA and protein syntheses and induced apoptosis which are likely major mechanisms whereby cytotoxicity is mediated.

Experimental Section

Melting points were determined on a Boetius apparatus at a heating rate of 4 °C/min and are uncorrected. Elemental analyses (C, H), performed at the former Chemistry Division of the Central Research Laboratory, Pécs, Hungary, and at the Organic Chemistry Department, Eötvös Loránd University, Budapest, Hungary, were undertaken on **1b**,**h**, **2f**,**h**,**j**,**l**, **3b**,**d**,**h**,**i**,**n**, and **4b**−**n** and were within 0.4% of the calculated values. The remaining compounds have been described previously and had melting points in accord with the literature values. Column chromatography was undertaken using Merck Kieselgel 60 and an eluting solvent of benzene or benzene:hexane, 1:1 (**4l**,**m**). The purity of the compounds was checked by TLC using Merck silica gel 60 F254 alumina sheets using both benzene and benzene:ethanol (4:1) as developing solvents for each compound. ^{1}H NMR spectra of all compounds were recorded in deuteriochloroform using a Perkin-Elmer R12 machine (60 MHz) and TMS as the internal standard. Infrared spectra of all compounds were recorded as potassium bromide disks or as films between potassium bromide disks using a Specord 75 instrument.

Synthesis of Series 1−3. The unsaturated ketones were prepared by a literature method[22] and purified by column chromatography followed by recrystallization from methanol. The melting points (°C) of unreported compounds are as follows: **1b**, 127−129; **1h**, 119−121; **2f**, 111−113; **2h**, 90−92; **2j**, 75−77; **2l**, 142−144; **3b**, 75−77; **3d**, 91−93; **3h**, 58−60; **3i**, 109−111; and **3n**, 177−179. The ^{1}H NMR spectra of representative compounds **1h**, **2h**, and **3h** were as follows: **1h**, δ 2.37(s, 3H, CH_3), 3.93 (d, 2H, J = 2.4 Hz, CH_2), 6.95−7.70 (m, 8H, aryl H), 7.75−8.05 (m, 1H, =CH); **2h**, δ 2.39 (s, 3H, CH_3), 2.75−3.35 (m, 4H, CH_2CH_2), 7.05−7.65 (m, 7H, aryl H), 7.86 (quasi s, 1H, =CH), 8.05−8.30 (m, 1H, aryl H); and **3h**, δ: 1.85−2.30 (m, 2H, 4-CH_2), 2.38 (s, 3H, CH_3), 2.30−3.05 (m, 4H, 3-CH_2 and 5-CH_2), 7.00−7.55 (m, 7H, aryl H), 7.65−7.95 (m, 2H, aryl H, =CH). The infrared spectra revealed cabonyl stretching frequencies for **1h**, **2h**, and **3h** at 1689, 1661, and 1659 cm^{-1}, respectively.

Synthesis of Series 4. The compounds were prepared by following literature procedures[22,23] and purified by column chromatography to give oils (**4b**,**d**,**f**,**h**,**j**,**k**) or solids (**4a**,**c**,**e**,**g**,**i**,**l**−**n**) which were crystallized from hexane. The melting points (°C) of the crystalline materials were as follows: **4a**, 39−41; **4c**, 67−69; **4e**, 80−82; **4g**, 91−93; **4i**, 50−51; **4l**, 53−55; **4m**, 91−93; and **4n**, 98−100. The ^{1}H NMR spectra of a representative compound **4h** was as follows: δ 1.45−1.95 (m, 6H, 4-CH_2, 5-CH_2, 6-CH_2), 2.37 (s, 3H, CH_3), 2.30−2.80 (m, 4H, 3-CH_2, 7-CH_2), 6.95−7.40 (m, 4H, aryl H), 7.50(quasi s, 1H, =CH). The infrared spectrum revealed a carbonyl stretching frequency of 1674 cm^{-1}.

Molecular Modeling. Models were built by the MacroModel Version 4.5 program[24,25] which was followed by a conformational search using the Monte Carlo method and MM2 force-field parameters to obtain minimum energy conformations.

X-ray Crystallography of 3i,k−n. The compounds were crystallized from methanol (**3i**,**k**,**m**,**n**) or hexane−diethyl ether by vapor diffusion (**3l**). A Nonius CAD-4 diffractometer with a ω scan was used for data collection, and the structure was solved by direct methods using NRCVAX[26] and refined using SHELXL-93.[27] Atomic scattering factors were taken from the literature.[28] All non-hydrogen atoms were found on the E-map and refined anisotropically. Hydrogen atom positions were calculated and not refined.

Statistical Analyses. The σ, π, and MR values were taken from the literature.[29] The p values obtained from linear (l) and semilogarithmic (sl) plots are given below, and the figures in parentheses refer to the plots of cytotoxicity against the σ, π, and MR constants, respectively: $P388_l$ (0.098, 0.559, 0.248), $P388_{sl}$ (0.019, 0.517, 0.081), $L1210_l$ (0.073, 0.758, 0.003), $L1210_{sl}$ (0.013, 0.472, 0.035), Molt $4/C8_l$ (0.480, 0.311, 0.060), Molt $4/C8_{sl}$ (0.236, 0.166, 0.120), CEM_l (0.509, 0.707, 0.014), CEM_{sl} (0.179, 0.323, 0.093), human $tumors_l$ (0.051, 0.332, 0.727), and human $tumors_{sl}$ (0.021, 0.862, 0.154).

Cytotoxicity Evaluations. The murine P388 screen was undertaken using a literature protocol.[30] The method employed for evaluating the compounds against murine L1210 cells as well as human Molt 4/C8 and CEM T-lymphocytes has been described previously.[31] The human tumor assay was conducted using a reported protocol.[32] In this test, the number of cell lines whose growth was inhibited by 50% or more at the maximum concentration of compound (log 10^{-4} M per total number of cell lines used) was as follows: **1f**, 46/55; **1l**, 12/55; **2f**, 55/55; **3a**, 55/55; **3b**, 56/56; **3d**, 56/56; **3e**, 56/56; **3h**, 55/55; **3i**, 55/55; **3j**, 55/55; **3k**, 42/42; **3l**, 56/56; **3m**, 10/56; **3n**, 46/47; **4a**, 10/54; **4b**, 29/53; **4c**, 19/54; **4d**, 43/52; **4e**, 52/53; **4h**, 6/55; **4i**, 2/55; **4j**, 13/53; **4k**, 0/57; **4l**, 51/52; **4m**, 52/52; **4n**, 16/51; and melphalan, 57/57.

Measurement of the Inhibition of RNA and Protein Syntheses and Apoptotic Indices in Jurkat T Cells. Inhibition of RNA and protein syntheses was determined by a literature procedure using Jurkat T cells.[33] The cytotoxicity and apoptosis studies followed a method previously employed in this laboratory[21] except that nigrosin dye was used in place of trypan blue in the cytotoxicity experiments and a solution of ethidium bromide (0.1% w/v) and acridine orange (0.1% w/v) was employed for the measurement of apoptosis.

Acknowledgment. Funding for this study was provided by CoCensys, Inc., to J. R. Dimmock, the Natural Sciences and Engineering Research Council of Canada to J. W. Quail and A. J. Nazarali, the National Cancer Institute of Canada to T. M. Allen, and the Belgian Fonds voor Geneeskundig Wetenschappelijk Onderzoek to J. Balzarini and E. De Clercq. The National Cancer Institute evaluated various compounds against the human tumor cell lines. Thanks are also given to Z. Dziadyk and S. Thiessen who typed a number of drafts of this manuscript.

Supporting Information Available: Crystal data, atomic coordinates, equivalent isotropic displacement parameters, bond lengths, anisotropic displacement parameters, hydrogen coordinates, isotropic displacement parameters, and torsion angles for **3i**,**k**−**n**. This information is available free of charge via the Internet at http://pubs.acs.org.

References

(1) Dimmock, J. R.; Kumar, P. Anticancer and cytotoxic properties of Mannich bases. *Curr. Med. Chem.* **1997**, *4*, 1−22.
(2) Dimmock, J. R.; Kandepu, N. M.; Hetherington, M.; Quail, J. W.; Pugazhenthi, U.; Sudom, A. M.; Chamankhah, M.; Rose, P.; Pass, E.; Allen, T. M.; Halleran, S.; Szydlowski, J.; Mutus, B.; Tannous, M.; Manavathu, E. K.; Myers, T. G.; De Clercq, E.; Balzarini, J. Cytotoxic activities of Mannich bases of chalcones and related compounds. *J. Med. Chem.* **1998**, *41*, 1014−1026.
(3) Mutus, B.; Wagner, J. D.; Talpas, C. J.; Dimmock, J. R.; Phillips, O. A.; Reid, R. S. 1-*p*-Chlorophenyl-4,4-dimethyl-5-diethylamino-1-penten-3-one hydrobromide, a sulfhydryl-specific compound which reacts irreversibly with protein thiols but reversibly with small molecular weight thiols. *Anal. Biochem.* **1989**, *177*, 237−243.
(4) Dimmock, J. R.; Raghavan, S. K.; Logan, D. M.; Bigam, G. E. Antileukemic evaluation of some Mannich bases derived from 2-arylidene-1,3-diketones. *Eur. J. Med. Chem.* **1983**, *18*, 248−254.
(5) Benvenuto, J. A.; Connor, T. A.; Monteith, D. K.; Laidlaw, J. L.; Adams, S. C.; Matney, T. S.; Theiss, J. C. Degradation and inactivation of antitumor drugs. *J. Pharm. Sci.* **1993**, *82*, 988−991.
(6) Dhar, D. N. *The chemistry of chalcones and related compounds*; John Wiley and Sons: New York, 1981; pp 224−225.
(7) Yit, C. C.; Das, N. P. Cytotoxic effect of butein on human colon adenocarcinoma cell proliferation. *Cancer Lett.* **1994**, *82*, 65−72.
(8) Wattenberg, L. W.; Coccia, J. B.; Galhaith, A. R. Inhibition of carcinogen-induced pulmonary and mammary carcinogenesis by chalcone administered after carcinogen exposure. *Cancer Lett.* **1994**, *83*, 165−169.
(9) Craig, P. N. Interdependence between physical parameters and selection of substituent groups for correlation studies. *J. Med. Chem.* **1971**, *14*, 680−684.
(10) Imbach, J.-L.; Pohland, A. E.; Weiler, E. D.; Cromwell, N. H. Nuclear magnetic resonance spectra of derivatives of various substituted indanones and tetralones. *Tetrahedron* **1967**, *23*, 3931−3941.
(11) Kevill, D. N.; Weiler, E. D.; Cromwell, N. H. Cis−trans isomerism of exocyclic α,β-unsaturated indanones and tetralones. *J. Org. Chem.* **1964**, *29*, 1276−1278.
(12) Orlov, V. D.; Borovoi, I. A.; Lavrushin, V. F. Structure of molecules of arylideneindanones, − tetralones and − chromanones. *Zh. Strukt. Khim.* **1976**, *17*, 691−697; *Chem. Abstr.* **1977**, *86*, 89056u.
(13) Hassner, A.; Mead, T. C. The stereochemistry of 2-benzalcyclohexanones and 2-benzalcyclopentanones. *Tetrahedron* **1964**, *20*, 2201−2210.
(14) Perjési, P.; Nusser, T.; Tarczay, Gy.; Sohár, P. E-2-Benzylidenebenzocycloalkanones. Stereostructure and NMR spectroscopic investigation. *J. Mol. Struct.*, in press.
(15) Sohár, P.; Perjési, P. Unpublished results.
(16) Boyd, M. R.; Paull, K. D. Some practical considerations and applications of the National Cancer Institute in vitro anticancer drug discovery screen. *Drug Dev. Res.* **1995**, *34*, 91−109.
(17) Grever, M. R.; Schepartz, S. A.; Chabner, B. A. The National Cancer Institute: Cancer drug discovery and development program. *Semin. Oncol.* **1992**, *19*, 622−638.
(18) Foye, W. O.; Sengupta, S. K. Cancer chemotherapy. In *Principles of Medicinal Chemistry*, 4th ed.; Foye, W. O., Lemke, T. L., Williams, D. A., Eds.; Williams and Wilkins: Media, PA, 1995; p 829.
(19) Tsurusawa, M.; Saeki, K.; Fujimoto, T. Differential induction of apoptosis on human lymphoblastic leukemia Nalm-6 and Molt-4 cells by various antitumor drugs. *Int. J. Hematol.* **1997**, *66*, 79−88.
(20) Chu, G. Cellular responses to cisplatin. *J. Biol. Chem.* **1994**, *269*, 787−790.
(21) Vashishtha, S. C.; Nazarali, A. J.; Dimmock, J. R. Application of fluorescence microscopy to measure apoptosis in Jurkat T cells after treatment with a new investigational anticancer agent (1213). *Cell. Mol. Neurobiol.* **1998**, *18*, 437−445.
(22) Neilsen, A. T.; Houlihan, W. J. The aldol condensation. In *Organic Reactions;* Cope, A. C., Ed.; John Wiley and Sons: New York, 1968; Vol. 16.
(23) Hickmott, P. W. Enamines: recent advances in synthetic, spectroscopic, mechanistic, and stereochemical aspects − I. *Tetrahedron* **1982**, *38*, 1975−2050.
(24) MacroModel, version 4.5; Department of Chemistry, Columbia University: New York, August 1994.

(25) Mohamadi, F.; Richards, N. G. J.; Guide, W. C.; Liskamp, M. L.; Caufield, C.; Chang, G.; Hendrikson, T.; Still, W. C. Macro-Model − An integrated software system for modeling organic and bioorganic molecules using molecular mechanics. *J. Comput. Chem.* **1990**, *11*, 440−467.
(26) Gabe, E. J.; LePage, Y.; Charland, J. P.; Lee, F. L.; White, P. S. An interactive program system for structure analyses. *J. Appl. Crystallogr.* **1989**, *22*, 384−387.
(27) Sheldrick, G. M. SHELXL-93, Program for the Refinement of Crystal Structures; University of Göttingen: Germany, 1993.
(28) *International Tables for X-ray crystallography*; Kynoch Press: Birmingham, 1974; Vol. IV.
(29) Hansch, C.; Leo, A. J. *Substituent Constants for Correlation Analysis in Chemistry and Biology*; John Wiley and Sons: New York, 1979; pp 49, 50.
(30) Phillips, O. A.; Nelson, L. A.; Knaus, E. E.; Allen, T. M.; Fathi-Afshar, R. Synthesis and cytotoxic activity of pyridylthio, pyridylsulfinyl and pyridosulfonyl methyl acrylates. *Drug Des. Deliv.* **1989**, *4*, 121−127.
(31) Balzarini, J.; De Clercq, E.; Mertes, M. P.; Shugar, D.; Torrence, P. F. 5-Substituted 2-deoxyuridines; correlation between inhibition of tumor cell growth and inhibition of thymidine kinase and thymidylate synthetase. *Biochem. Pharmacol.* **1982**, *31*, 3673−3682.
(32) Boyd, M. R. In *Cancer: Principles and Practice of Oncology Update*; DeVita, V. T., Jr., Hellman, S., Rosenberg, S. A., Eds.; J. B. Lippincott: Philadelphia, 1989; Vol. 3, No. 10, pp 1−12.
(33) Martin, S. J.; Lennon, S. V.; Bonham, A. M.; Cotter, T. G. Induction of apoptosis (programmed cell death) in human leukemic HL-60 cells by inhibition of RNA and protein synthesis. *J. Immunol.* **1990**, *145*, 1859−1867.

JM9806695